cell collection on the CS-3000+ and Amicus blood cell separators. *Transfusion* 43: 1423–1427.

14. Kajiume, T., Kawano, Y., Takaue, Y., Abe, T., Okamoto, Y., Makimoto, A., Watanabe, T., Sato, J., Yokobayashi, A., and Kuroda, Y. 1998. Continuous monitoring of hematocrit values during apheresis for allogeneic peripheral blood stem cell collection. *J. Hematother.* 7: 493–497.
15. Kanold, J., Halle, P., Rapatel, C., Berger, M., Gembara, P., de Lumley, L., Vannier, J.P., Lutz, P., Plantaz, D., Malpuech, G., and Demeocq, F. 1998. Safe and efficient peripheral blood stem cell collection in the smallest of children. *Ther. Apher.* 2: 49–57.
16. Kessinger, A., Armitage, J.O., Smith, D.M., Landmark, J.D., Bierman, P.J., and Weisenburger, D.D. 1989. High-dose therapy and autologous peripheral blood stem cell transplantation for patients with lymphoma. *Blood* 74: 1260–1265.
17. Korbling, M., Przepiorka, D., Huh, Y.O., Engel, H., van Besien, K., Giralt, S., Andersson, B., Kleine, H.D., Seong, D., Deisseroth, A.B., Andreeff, M., and Champlin, R. 1995. Allogeneic blood stem cell transplantation for refractory leukemia and lymphoma: potential advantage of blood over marrow allografts. *Blood* 85: 1659–1665.
18. Nash, K., Chang, Q., Watts, A., Treter, S., Oravec, G., Ferrara, V., Buhler, L., Basker, M., Gojo, S., Sachs, D.H., White-Scharf, M., Down, J.D., and Cooper, D.K. 1999. Peripheral blood progenitor cell mobilization and leukapheresis in pigs. *Lab. Anim. Sci.* 49: 645–649.
19. Negrin, R.S., Atkinson, K., Leemhuis, T., Hanania, E., Juttner, C., Tierney, K., Hu, W.W., Johnston, L.J., Shizurn, J.A., Stockerl-Goldstein, K.E., Blume, K.G., Weisman, I.L., Bower, S., Baynes, R., Dansey, R., Karanes, C., Peters, W., and Klein, J. 2000. Transplantation of highly purified $CD34^+Thy\text{-}1^+$ hematopoietic stem cells in patients with metastatic breast cancer. *Biol. Blood Marrow Transplant.* 6: 262–271.
20. Norol, F., Merlet, P., Isnard, R., Sebillon, P., Bonnet, N., Cailliot, C., Carrion, C., Ribeiro, M., Charlotte, F., Pradeau, P., Mayol, J.F., Peinnequin, A., Drouet, M., Safsafi, K., Vernant, J.P., and Herodin, F. 2003. Influence of mobilized stem cells on myocardial infarct repair in a nonhuman primate model. *Blood* 102: 4361–4368.
21. Primate Society of Japan. 1986. Guiding Principles for Animal Experiments Using Nonhuman Primates. *Primate Res.* 2: 111–113.
22. Rosenfeld, C.S. 1993. A strategy for processing of peripheral blood stem cells utilizing the small volume collection chamber and cryopreservation without a rate controller using pentastarch. *J. Hematother.* 2: 525–528.
23. Rowley, S.D., Prather, K., Bui, K.T., Appel, M., Felt, T., and Bensinger, W.I. 1999. Collection of peripheral blood progenitor cells with an automated leukapheresis system. *Transfusion* 39: 1200–1206.
24. Schmitz, N., Dreger, P., Suttorp, M., Rohwedder, E.B., Haferlach, T., Loffler, H., Hunter, A., and Russell, N.H. 1995. Primary transplantation of allogeneic peripheral blood progenitor cells mobilized by filgrastim (granulocyte colony-stimulating factor). *Blood* 85: 1666–1672.
25. Schwella, N., Movassaghi, K., Scheding, S., Ahrens, N., and Salama, A. 2003. Comparison of two leukapheresis programs for computerized collection of blood progenitor cells on a new cell separator. *Transfusion* 43: 58–64.
26. Shibata, H., Hanazono, Y., Ageyama, N., Nagashima, T., Ueda, Y., Hasegawa, M., Ozawa, K., Yoshikawa, Y., and Terao, K. 2003. Collection and analysis of hematopoietic progenitor cells from cynomolgus macaques (*Macaca fascicularis*): assessment of cross-reacting monoclonal antibodies. *Am. J. Primatol.* 61: 3–12.
27. Snyder, E.L., Baril, L., Cooper, D.L., Min, K., Mechanic, S., Stoddart, L., Burtness, B., Seagraves, P., Debelak, J., Gudino, M., and McCullough, J. 2000. *In vitro* collection and posttransfusion engraftment characteristics of MNCs obtained by using a new separator for autologous PBPC transplantation. *Transfusion* 40: 961–967.
28. Sohn, S.K., Kim, J.G., Chae, Y.S., Kim, D.H., Lee, N.Y., Suh, J.S., and Lee, K.B. 2003. Large-volume leukapheresis using femoral venous access for harvesting peripheral blood stem cells with the Fenwal CS 3000 Plus from normal healthy donors: predictors of $CD34^+$ cell yield and collection efficiency. *J. Clin. Apher.* 18: 10–15.
29. Stamm, C., Westphal, B., Kleine, H.D., Petzsch, M., Kittner, C., Klinge, H., Schumichen, C., Nienaber, C.A., Freund, M., and Steinhoff, G. 2003. Autologous bone-marrow stem-cell transplantation for myocardial regeneration. *Lancet* 361: 45–46.
30. Ueda, K., Hanazono, Y., Shibata, H., Ageyama, N., Ueda, Y., Ogata, S., Tabata, T., Nagashima, T., Takatoku, M., Kume, A., Ikehara, S., Taniwaki, M., Terao, K., Hasegawa, M., and Ozawa, K. 2004. High-level *in vivo* gene marking after gene-modified autologous hematopoietic stem cell transplantation without marrow conditioning in nonhuman primates. *Mol. Ther.* 10: 469–477.
31. Witt, V., Fischmeister, G., Scharner, D., Printz, D., Pottschger, U., Fritsch, G., and Gadner, H. 2001. Collection efficiencies of MNC subpopulations during autologous $CD34^+$ peripheral blood progenitor cell (PBPC) harvests in small children and adolescents. *J. Clin. Apher.* 16: 161–168.
32. Woloskie, S., Armelagos, H., Meade, J.M., and Haas, D. 2001. Leukodepletion for acute lymphocytic leukemia in a three-week-old infant. *J. Clin. Apher.* 16: 31–32.
33. Yoshino, N., Ami, Y., Terao, K., Tashiro, F., and Honda, M. 2000. Upgrading of flow cytometric analysis for absolute counts, cytokines and other antigenic molecules of cynomolgus monkeys (*Macaca fascicularis*) by using anti-human cross-reactive antibodies. *Exp. Anim.* 49: 97–110.
34. Yoshioka, T., Ageyama, N., Shibata, H., Yasu, T., Misawa, Y., Takeuchi, K., Matsui, K., Yamamoto, K., Terao, K., Shimada, K., Ikeda, U., Ozawa, K., and Hanazono, Y. 2005. Repair of infarcted myocardium mediated by transplanted bone marrow-derived $CD34^+$ stem cells in a nonhuman primate model. *Stem Cells* 23: 355–364.

STEM CELLS®
Original Article

Repair of Infarcted Myocardium Mediated by Transplanted Bone Marrow–Derived CD34+ Stem Cells in a Nonhuman Primate Model

TORU YOSHIOKA[a,c] NAOHIDE AGEYAMA,[f] HIROAKI SHIBATA,[a,f] TAKANORI YASU,[c] YOSHIO MISAWA,[d] KOICHI TAKEUCHI,[e] KEIJI MATSUI,[c] KEIJI YAMAMOTO,[c] KEIJI TERAO,[f] KAZUYUKI SHIMADA,[c] UICHI IKEDA,[g] KEIYA OZAWA,[a,b] YUTAKA HANAZONO[a]

[a]Center for Molecular Medicine; [b]Division of Hematology, and [c]Division of Cardiology, Department of Internal Medicine; [d]Division of Cardiovascular Surgery, Department of Surgery; and [e]Department of Anatomy, Jichi Medical School, Minamikawachi, Tochigi; [f]Tsukuba Primate Center, National Institute of Infectious Diseases, Tsukuba, Ibaraki; [g]Department of Organ Regeneration, Shinshu University Graduate School of Medicine, Matsumoto, Nagano, Japan

Key Words. Nonhuman primate • Acute myocardial infarction • Stem cell transplantation Genetic marking • Lentivirus vector • Plasticity • Neoangiogenesis

ABSTRACT

Rodent and human clinical studies have shown that transplantation of bone marrow stem cells to the ischemic myocardium results in improved cardiac function. In this study, cynomolgus monkey acute myocardial infarction was generated by ligating the left anterior descending artery, and autologous CD34+ cells were transplanted to the peri-ischemic zone. To track the in vivo fate of transplanted cells, CD34+ cells were genetically marked with green fluorescent protein (GFP) using a lentivirus vector before transplantation (marking efficiency, 41% on average). The group receiving cells ($n = 4$) demonstrated improved regional blood flow and cardiac function compared with the saline-treated group ($n = 4$) at 2 weeks after transplant. However, very few transplanted cell–derived, GFP-positive cells were found incorporated into the vascular structure, and GFP-positive cardiomyocytes were not detected in the repaired tissue. On the other hand, cultured CD34+ cells were found to secrete vascular endothelial growth factor (VEGF), and the in vivo regional VEGF levels showed a significant increase after the transplantation. These results suggest that the improvement is not the result of generation of transplanted cell–derived endothelial cells or cardiomyocytes; and raise the possibility that angiogenic cytokines secreted from transplanted cells potentiate angiogenic activity of endogenous cells.
STEM CELLS *2005;23:355–364*

INTRODUCTION

Recent clinical studies have shown that the introduction of bone marrow cells can restore blood flow in ischemic myocardium and ameliorate cardiac function [1–6]. Despite enthusiasm for these studies, it is unclear how transplanted bone marrow cells contribute to the clinical improvement. Because endothelial progenitor cells are identified in bone marrow cells [7], these cells might participate in the repair

Correspondence: Yutaka Hanazono, M.D., Ph.D., Division of Regenerative Medicine, Center for Molecular Medicine, Jichi Medical School, 3311-1 Yakushiji, Minamikawachi, Tochigi 329-0498, Japan. Telephone: 81-285-58-7450; Fax: 81-285-44-5205; e-mail: hanazono@jichi.ac.jp Received August 16, 2004; accepted for publication November 30, 2004. 1066-5099/2005/$12.00/0 doi: 10.1634/stemcells.2004-0200

of vascular tissue. On the other hand, it has been reported that hematopoietic stem cells differentiate into endothelial cells and cardiomyocytes when transplanted into the ischemic myocardium in mice [8]. More recently, however, it has been reported that hematopoietic stem cells do not give rise to nonhematopoietic cells in the ischemic myocardium in murine models [9–11].

In vivo tracking and plastic properties of hematopoietic stem or progenitor cells have not been examined in primate cardiac ischemia. We have transplanted genetically marked autologous CD34+ cells to the ischemic myocardium in a nonhuman primate (cynomolgus macaque) model and tracked the in vivo fate of the cells. We have used CD34+ cells because the cells are widely used as a fraction of hematopoietic stem cells in clinical and nonhuman primate studies [12]. In addition, CD34+ cells contain vascular endothelial progenitor cells [7]. Thus, the present study can address the question of whether transplanted CD34+ cells really give rise to endothelial cells and cardiomyocytes in ischemic myocardium in primates.

Materials and Methods

Animals

Eight cynomolgus macaques bred in the Tsukuba Primate Center (Ibaraki, Japan) were enrolled in the present study. This study strictly adhered to the rules for animal care and management of the Tsukuba Primate Center, as well as the guiding principles for animal experiments using nonhuman primates formulated by the Primate Society of Japan. The protocols of animal experiments were approved by the animal welfare and animal care committee of the National Institute of Infectious Diseases (Tokyo).

Preparation of CD34+ Cells

Cynomolgus bone marrow (50 ml) was aspirated from the iliac crest under an isoflurane-induced general anesthesia. From the bone marrow, a nucleated cell fraction was obtained after red blood cell lysis with addition of ACK buffer (Biosource, Camarillo, CA). CD34+ cells were isolated using magnetic beads conjugated with anti-human CD34 (clone 561; Dynal, Lake Success, NY), which cross-reacts with cynomolgus CD34 [13]. The purity of CD34+ cells at harvest ranged from 90% to 95%, as assessed with another anti-human CD34 (clone 563; PharMingen, San Diego) that cross-reacts with cynomolgus CD34 [13]. The purity remained at the same levels after the 1-day transduction culture, which is discussed next.

Lentiviral Transduction

A simian immunodeficiency virus (SIV)-based lentivirus vector carrying enhanced jellyfish green fluorescent protein (GFP) (Clontech, Palo Alto, CA) was used for transduction. The vector was prepared as previously reported [14, 15]. All recombinant DNA experiments were approved by the Ministry of Education, Culture, Sports, Science and Technology of Japan.

CD34+ cells (1×10^6) were seeded in six-well plates in 2 ml of StemSpan serum-free expansion medium (Stem Cell Technologies, Vancouver) supplemented with recombinant human thrombopoietin (100 ng/ml; Kirin, Tokyo), recombinant human stem cell factor (100 ng/ml; Biosource, Camarillo, CA), recombinant human Flt-3 ligand (100 ng/ml; Research Diagnostics, Flanders, NJ), and antibiotics (100 U/ml of penicillin and 0.1 μg/ml of streptomycin; Meiji, Tokyo). The cells were transduced twice each for 12 hours (total, 24 hours) with the SIV vector at 50 transducing units per target cell. After transduction, cells were cryopreserved with 10% dimethylsulfoxide (Wako, Osaka, Japan) and 1% Dextran 40 (Yoshitomi, Osaka, Japan) in a controlled-rate programmable freezer (Kryo 10; Planer Biomed, Middlesex, UK) until transplantation. The viability of cells after thawing was 53.0 ± 6.5%, as assessed by trypan blue staining. An aliquot of transduced cells was assessed for GFP expression at 48 hours after transduction by flow cytometry using a FACScan (Becton Dickinson, Franklin Lakes, NJ) with excitation at 488 nm and fluorescence detection at 530 ± 30 nm.

In Vitro Endothelial Differentiation

CD34+ cells were seeded on fibronectin-coated plates (Becton Dickinson) in M199 medium (Invitrogen, Carlsbad, CA) with 20% fetal calf serum and bovine pituitary extracts (Invitrogen) as previously described [7]. After 7 days in culture, cells were examined for the uptake of DiI-acetylated low-density lipoprotein (LDL) and for the expression of CD31, von Willebrand factor (vWF), vascular endothelial (VE)-cadherin, and vascular endothelial growth factor receptor (VEGFR)-2. Briefly, adherent cells were incubated with 1 μg/ml of DiI-acetylated LDL (Molecular Probes, Eugene, OR) for 4 hours at 37°C. For immunofluorescence staining, after fixation in ice-cold 4% paraformaldehyde for 10 minutes and blocking in 1% bovine serum albumin (BSA) for 15 minutes, cells were incubated with a primary antibody: mouse anti-human CD31 (VM-59; Becton Dickinson), rabbit anti-human vWF (DakoCytomation, Glostrup, Denmark), mouse anti-human VE-cadherin (55-7H1; Becton Dickinson), or rabbit anti-mouse VEGFR2 (Santa Cruz Biotechnology, Santa Cruz, CA) for 1 hour at room

temperature. Cells were then incubated with a secondary antibody, Texas red–conjugated horse anti-mouse immunoglobulin G (IgG) (Vector, Burlingame, CA) or goat anti-rabbit IgG (Vector) for 30 minutes at room temperature.

Myocardial Infarction and Transplantation

All operations on cynomolgus monkeys were performed under an isoflurane-induced general anesthesia. Thoracotomy was conducted, the pericardium was opened, and the left anterior descending coronary artery was ligated with 5-0 prolene sutures. One to 2 hours after the ligation, GFP-transduced, autologous $CD34^+$ cells in normal saline were injected with a microsyringe through a 27-gauge needle into 10 sites (5 μl/site) in the peri-ischemic zone. In the control group, saline alone was injected in the same way. The pericardium and chest were closed. The animals then received butorphanol tartrate (0.5 mg/kg, intramuscularly) daily for 5 days to alleviate the pain associated with the operation and myocardial infarction.

Echocardiography

Echocardiographic imaging was obtained using a Sonos 5500 system (Philips Medical Systems, Andover, MA) before transplantation and at 2 weeks after transplant. The echocardiography was conducted by independent technicians irrelevant to our study group. In one animal (BM97080), it was additionally performed at 12 weeks. Short-axis two-dimensional images at the midpapillary level of the left ventricle were stored, and percent fractional shortening (%FS) was calculated to assess cardiac function.

Myocardial contrast echocardiography (MCE) was performed at day 0 (just before transplantation) and at 2 weeks after transplant to assess regional blood flow and blood flow defect size. In one animal (BM97080), chronic assessment was performed at 12 weeks after transplant. The electrocardiograph-triggered end-systolic intermittent imaging was conducted in short-axis views at incremental pulsing intervals (triggering intervals of 1, 2, 3, 4, and 8 beats) using an S12 probe. Once optimized, the settings of depth (4 cm), mechanical index (0.9), and focus (3 cm) were fixed. The contrast agent (perflutren; Yamanouchi, Tokyo) consisted of lipid-coated microbubbles of perfluorocarbon [16]. Perflutren diluted with saline (1:10) was administered intravenously at a constant rate (0.01 ml/kg per min). For the assessment of regional blood flow, MCE images were analyzed using ORIGIN 6.0J (Lightstone, Tokyo), and the blood flow was calculated as previously described [17]. Data are presented as a blood flow ratio (the peri-infarct versus nonischemic control region or the infarct versus nonischemic control region). For the assessment of blood flow defect, MCE images obtained at triggering interval of four beats were analyzed using National Institutes of Health Image software (version 1.61). Data are presented as percent defect compared with the total blood flow.

Microspheres

Colored microspheres (15 μm ± 2% diameter; E-Z Trac, Los Angeles) were used to evaluate regional blood flow 2 weeks after transplant [18], with the exception of one animal (BM97080), in which evaluation was performed 12 weeks after transplant. A set of microspheres (2×10^6) was diluted in 2 ml of saline and injected into the left ventricle over 30 seconds. A reference blood sample was withdrawn at a constant rate of 5 ml/min through the femoral artery. After the collection of blood samples, monkeys were irrigated with saline for mercy killing and blood was completely washed out. The heart was excised from each monkey. Tissue samples from the infarct, peri-infarct, and nonischemic regions (one sample per region) were digested, microspheres were collected, and the blood flow was calculated according to the manufacturer's instructions. Data are presented as blood flow ratio (the peri-infarct versus nonischemic control region or the infarct versus nonischemic control region).

Immunohistochemistry

Tissue samples from the infarct, peri-infarct, and nonischemic regions at 2 weeks after transplant were embedded in optimal cutting temperature compound (Sakura, Zoeterwoude, Netherlands) and frozen in liquid nitrogen. Sections were prepared (6 μm), fixed for 10 minutes at 4°C in 4% paraformaldehyde in phosphate-buffered saline (PBS), and blocked with 1% BSA in PBS. The sections were incubated at room temperature with a primary antibody, monoclonal mouse anti-human CD31 (1:200; Becton Dickinson), followed by a secondary antibody, biotin-conjugated horse anti-mouse IgG (1:500; Vector). The sections were then treated with avidin-alkaline phosphatase (ABC AP kit; Vector) for 30 minutes. The reaction was developed with a Vector Red substrate kit (SK-5100; Vector). In the case of double staining of CD31 and GFP, the above sections were further incubated with polyclonal rabbit anti-GFP (1:200; Clontech) followed by biotin-conjugated anti-rabbit IgG (1:500; Vector) and treated with avidin-peroxidase (ABC Elite kit; Vector). The reaction was developed with a Vector SG substrate kit (SK-4700; Vector). The sections were counterstained with hematoxylin, mounted in glycerol, and examined under a light microscope.

In Situ Polymerase Chain Reaction

In situ detection of transduced cell progeny was performed by amplifying proviral sequences as previously reported [19]. The following primer set for the GFP gene was used:

5'-CGT CCA GGA GCG CAC CAT CTT C-3' and 5'-GGT CTT TGC TCA GGG CGG ACT-3'. The polymerase chain reaction (PCR) mixture consisted of 420 μM dATP, 420 μM dCTP, 420 μM dGTP, 378 μM dTTP, 42 μM digoxigenin-labeled dUTP (Roche, Mannheim, Germany), 0.8 μM of each GFP primer, 4.5 mM $MgCl_2$, 1 × PCR buffer (Mg^{2+} free), and 4 U of Takara Taq DNA polymerase (Takara, Kyote). Sections were prepared with a Takara slide frame (Takara) from the infarct, peri-infarct, and nonischemic regions at 2 weeks after transplant. PCR was performed using a PTC100 thermal cycler (MJ Research, Watertown, MA) with the following conditions: 94°C for 1 minute and 57°C for 1 minute with 10 cycles. The digoxigenin-incorporated DNA fragments were detected using horseradish peroxidase (HRP)-conjugated rabbit F(ab') anti-digoxigenin antibody (DakoCytomation). The sections were then stained for HRP using a Vector SG substrate kit (Vector). Finally, the sections were counterstained with a Kernechtrot solution (Muto, Tokyo) that stains nucleotides, mounted in glycerol, and examined under a light microscope.

ELISA

Vascular endothelial growth factor (VEGF) and basic fibroblast growth factor (bFGF) levels in tissue lysate or medium were assessed by ELISA (R&D Systems, Minneapolis) according to the manufacturer's instructions. Tissue lysate was obtained from the peri-infarct region (three samples from each monkey) at 2 weeks after transplant. Briefly, tissue was homogenized and suspended in lysis buffer containing 10 mM Tris-HCl (pH 8.0), 1% Nonidet P-40, 150 mM NaCl, and protease inhibitor cocktail tablets (Complete Mini, Roche). The suspension was rocked at 4°C for 20 minutes and centrifuged at 16,000g and 4°C for 30 minutes. The supernatant was used for ELISA. The protein concentration of lysate was determined with DC Protein Assay (Bio-Rad, Hercules, CA).

Results

Lentiviral Marking

The CD34+ fraction of autologous bone marrow cells was used for transplantation in our study (Table 1). Before transplantation, CD34+ cells were genetically marked with GFP using an SIV-based lentivirus vector. The ex vivo transduction results are summarized in Table 1. The transduced cells were frozen until transplantation. An aliquot of the transduced cells was examined in vitro for the endothelial differentiation ability. After the differentiation culture, a vessel-like structure was observed (Fig. 1A). The ability of cells to take up DiI-acetylated LDL and the expression of CD31, vWF, VE-cadherin, and VEGFR-2 suggested the endothelial lineage (Fig. 1B). We and others have already confirmed the ability of hematopoietic differentiation of the cells [20, 21]. Taken together, the SIV-mediated GFP gene transfer does not spoil the differentiation abilities of CD34+ cells. In addition, on average, 41% of cells fluoresced 48 hours after transduction, and 56% of

Table 1. Summary of ex vivo transduction and transplantation

	Sex	Age (y)	Body weight (kg)	Harvested bone marrow cell number	Isolated CD34+ cell number	Transplanted cell number	% GFP expression Before[a]	% GFP expression After[b]
Saline group								
CTR01061[c]	M	3	4.1			NA		
CTR99056	M	3	3.4					
CTR96116	F	5	3.2					
CTR99051	M	5	5.9					
CD34+ cell group								
BM01052	M	3	3.9	213×10^6	1.00×10^6	0.47×10^6	49	87
BM01051[d]	M	3	4.1	396×10^6	5.14×10^6	2.20×10^6	51	54
BM97080[e]	M	5	3.9	330×10^6	2.35×10^6	1.04×10^6	49	67
BM90047	M	13	5.8	343×10^6	3.10×10^6	1.07×10^6	16	14
Average		5	4.3	321×10^6	2.90×10^6	1.20×10^6	41	56

[a]Before endothelial differentiation of GFP-transduced CD34+ cells.
[b]After the in vitro endothelial differentiation.
[c]CTR01061 died of heart failure 5 days after myocardial infarction.
[d]BM01051 developed a ventricular aneurysm after myocardial infarction.
[e]BM97080 was killed 12 weeks after the treatment. All other animals were killed 2 weeks after the treatment.
Abbreviations: GFP, green fluorescent protein; NA, not applicable.

endothelial cells still fluoresced after in vitro differentiation (Table 1), showing that the GFP expression is stable during the in vitro differentiation to endothelial cells. Thus, GFP was expected to serve as a good genetic tag after transplantation.

Acute Myocardial Infarction and Autologous Transplantation

Cynomolgus acute myocardial infarction was generated by ligating the left anterior descending artery. One to two hours after the ligation, GFP-transduced, autologous CD34$^+$ cells were injected in the peri-ischemic zone at 10 sites (total, $1.20 \pm 0.73 \times 10^6$ cells; $n = 4$). In the control group, saline was injected in the same way ($n = 4$). We conducted contrast echocardiography immediately after the coronary ligation and found no significant differences in the blood flow defect size (percent blood flow defect compared with the total) between the cell-treated and saline-treated groups ($13.0 \pm 2.1\%$ versus $12.3 \pm 3.5\%$, $p = .75$), suggesting that the initial risk of infarction did not differ between the two groups. In addition, we tried to assess the cardiac isozyme of serum creatine kinase (CK) to evaluate the infarct size; however, either the immuno-inhibition assay or chemical luminescence immunoassay did not work well for cynomolgus monkey samples. We were at least able to show that total CK values at 24 hours after the ligation did not significantly differ between the two groups ($p = .83$).

One of the control monkeys (CTR01061) died of heart failure 5 days after myocardial infarction, and the other control monkeys showed a decrease in %FS at 2 weeks after infarction (Fig. 2). Thus, all four control animals showed the deteriorated cardiac function. In the cell-treated group, one monkey (*, BM01051) underwent ventricular fibrillation immediately after the ligation and survived after cardiopulmonary resuscitation but eventually developed a ventricular aneurysm. Only this animal showed a decrease in %FS despite CD34$^+$ cell treatment; the other animals receiving CD34$^+$ cells showed an increase in %FS (Fig. 2). CD34$^+$ cell treatment may not be able to rescue such a heavily impaired heart but otherwise had a significant effect on cardiac function. Even an old monkey (BM90047, Table 1) showed improved %FS.

The relative blood flow in the peri-infarct to nonischemic control region was also significantly ameliorated in the CD34$^+$ cell–treated monkeys compared with the saline-treated ones, as assessed using contrast echocardiography (Fig. 3A) and colored microspheres (Fig. 3B). An excellent correlation was found between the two methods (Fig. 3C; correlation coefficient = 0.93). Two groups (CD34$^+$ cell–treated and saline-treated) were well separated on the panel, showing an obvious positive effect of CD34$^+$ cell injection on the blood flow in the peri-infarct zone after acute myocardial infarction. In fact, the average myocardial blood flow in the peri-infarct region in the absolute value was 0.988 ml/g per minute and 0.383 ml/g per minute for the cell-treated and saline-treated groups, respectively. Of note, the blood flow in the peri-infarct zone was ameliorated even in the animal with a ventricular aneurysm. On the other hand, the relative blood flow in the infarct to nonischemic region did not show

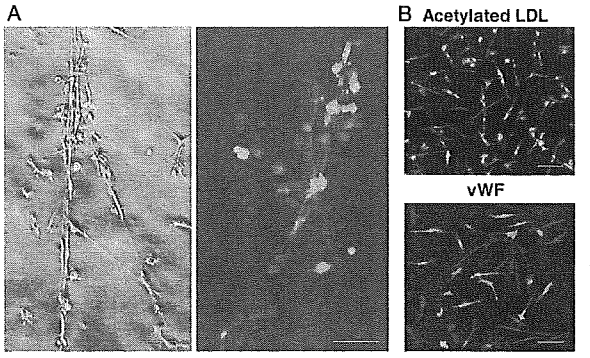

Figure 1. In vitro endothelial differentiation of cynomolgus CD34$^+$ cells lentivirally transduced with GFP. The transduced CD34$^+$ cells were differentiated to endothelial cells after 7 days in culture. **(A)**: Representative vessel-like structure derived from CD34$^+$ cells observed under a phase-contrast microscope (left) and a fluorescent microscope (right). **(B)**: The transduced CD34$^+$ cells differentiated into fluorescent cells (green) positive for the cellular intake of acetylated LDL and immunostaining for von Willebrand factor (vWF) (stained in red). Bar = 100 μm. Abbreviations: GFP, green fluorescent protein; LDL, low-density lipoprotein.

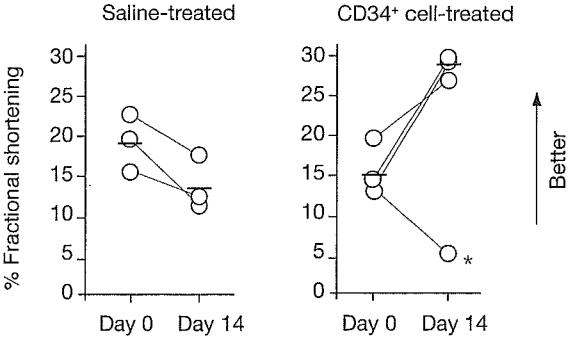

Figure 2. Improved cardiac function after CD34$^+$ cell transplantation. Cardiac function was assessed by echocardiography in terms of percent fractional shortening (%FS) before and 2 weeks after treatment. One monkey in the saline-treated group (CTR01061) died of heart failure 5 days after myocardial infarction and is not included in the figure. One monkey in the CD34$^+$ cell–treated group (*, BM01051) developed a left ventricular aneurysm after myocardial infarction. If this animal was excluded from the statistical analysis, the cardiac function was significantly improved in the CD34$^+$ cell–treated compared with the saline-treated group in terms of the ratio of %FS at day 14 versus day 0 after transplant ($p = .017$).

a significant difference between the CD34+ cell–treated and saline-treated groups. The peri-infarct region was the injection site, and thus the highest degree of change would be expected there.

All monkeys except one CD34+ cell–treated monkey (BM97080) were examined for cardiac function and blood flow at 2 weeks after transplantation, and their tissue sections were finally prepared at this time point (see below). BM97080 was examined at 12 weeks, at which time the cardiac function was still improved compared with immediately after infarction (data not shown) and the blood flow data were in a position similar to the cell-treated group at 2 weeks (Fig. 3C).

In Vivo Tracking of Transplanted Cells

Two weeks after the transplantation, tissue sections were prepared from the infarct, peri-infarct, and nonischemic regions. Immunostaining of an endothelial marker CD31 demonstrated more vessels in the peri-infarct region of the CD34+ cell-treated than saline-treated myocardium (Fig. 4A). In fact, the capillary density of the peri-infarct region was significantly better preserved in the cell-treated than saline-treated group, although there was no significant difference in the capillary density of the nonischemic control regions between the two groups (Fig. 4B).

Double immunostaining with anti-CD31 and anti-GFP showed that some cells in vessels were positive for both CD31 and GFP in the peri-infarct region (Fig. 5A). The result clearly indicates that at least some transplanted CD34+ cells gave rise to endothelial cells. However, we found that the transplanted cell progeny accounted for only a small fraction of endothelial cells after examining more than 100 sections of the peri-infarct region. In situ PCR for proviral GFP sequences also showed that few CD31-positive endothelial cells contained the GFP-provirus (Fig. 5B). There were no GFP-positive cardiomyocytes in more than 100 sections. Most of the transplanted cell progeny were found not incorporated in vessels (Fig. 5C). Hematoxylin-eosin staining did not show any noncardiac tissue regeneration in the myocardium.

On the other hand, we found that in vitro conditioned medium of CD34+ cell culture for endothelial differentiation contained high levels of VEGF, whereas unconditioned medium did not contain detectable VEGF, as assessed

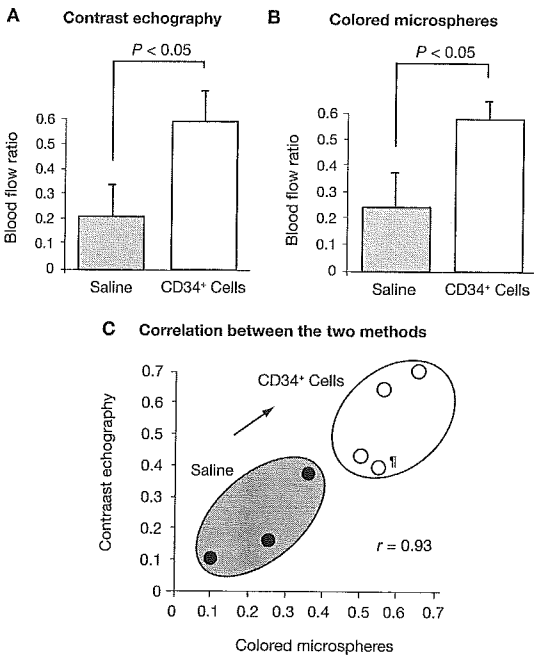

Figure 3. Improved regional blood flow after CD34+ cell transplantation. Myocardial contrast echocardiography (**A**) and colored microspheres (**B**) showed a significantly ameliorated blood flow ratio (the peri-infarct to nonischemic control region) in the CD34+ cell–treated monkeys ($n = 3$) compared with the saline-treated monkeys ($n = 3$) at 2 weeks after treatment. (**C**): An excellent correlation was found between the two methods. A CD34+ cell–treated monkey (¶, BM97080) that was examined at 12 weeks after transplant is included in the panel (**C**) but excluded from the statistical analysis in (**A**) and (**B**).

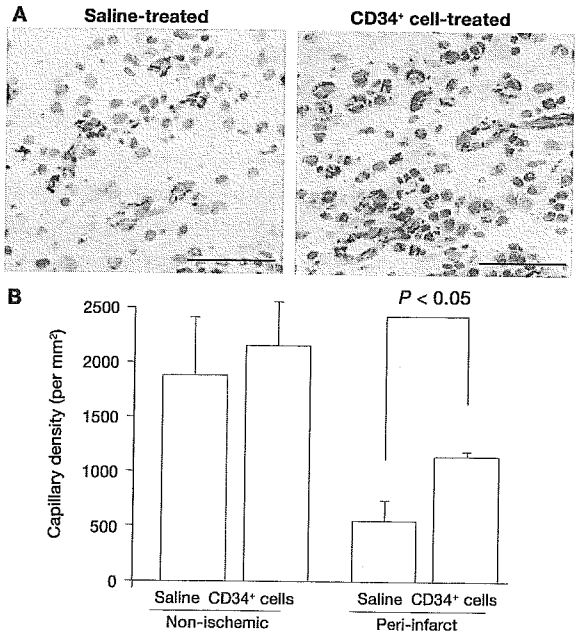

Figure 4. Neoangiogenesis in the ischemic myocardium. Tissue sections were prepared at 2 weeks after the treatment. (**A**): Representative results of immunostaining with anti-CD31 (stained in brown) in the peri-infarct region of the saline-treated and CD34+ cell–treated myocardium. Bar = 50 μm. (**B**): The density of CD31-positive capillaries in the peri-infarct and control nonischemic regions in the saline-treated and CD34+ cell–treated groups. Five fields for each section were randomly selected ($n = 3$ for the saline injection, $n = 3$ for the CD34+ cell injection), and the number of CD31-positive capillaries was counted (average ± standard deviation).

by ELISA (Fig. 6A). In addition, in vivo VEGF levels in the peri-infarct tissue were significantly higher in the CD34$^+$ cell–treated than saline-treated group (Fig. 6B, left), although in vivo levels of bFGF differed little between the two groups (Fig. 6B, right).

Discussion

Although gained with small numbers of cynomolgus monkeys, our data suggest that the direct transplantation of bone marrow CD34$^+$ cells, even without coronary bypass grafts or percutaneous coronary intervention, results in improved regional blood flow and cardiac function after myocardial infarction in nonhuman primates. Furthermore, we have tried to see the contribution of transplanted CD34$^+$ cells to the repair of ischemic myocardium. To this end, we genetically marked CD34$^+$ cells with GFP using an SIV-based lentiviral vector before transplantation. Lentiviral vectors can transduce nondividing cells unlike oncoretroviral vectors, and thus the ex vivo culture period with multiple cytokines to allow cell cycling can be reduced to 1 day or less [20, 22, 23]. This is the great advantage of using lentiviral vectors over oncoretroviral vectors for transduction of multipotent stem cells, given that extended ex vivo culture of stem cells may result in loss of multilineage differentiation and engraftment abilities [24]. Human immunodeficiency virus (HIV)-1–based lentiviral vectors can efficiently transduce human cells, but not Old World monkey cells [25]. According to a recent report, a species-specific cytoplasmic component confers the innate

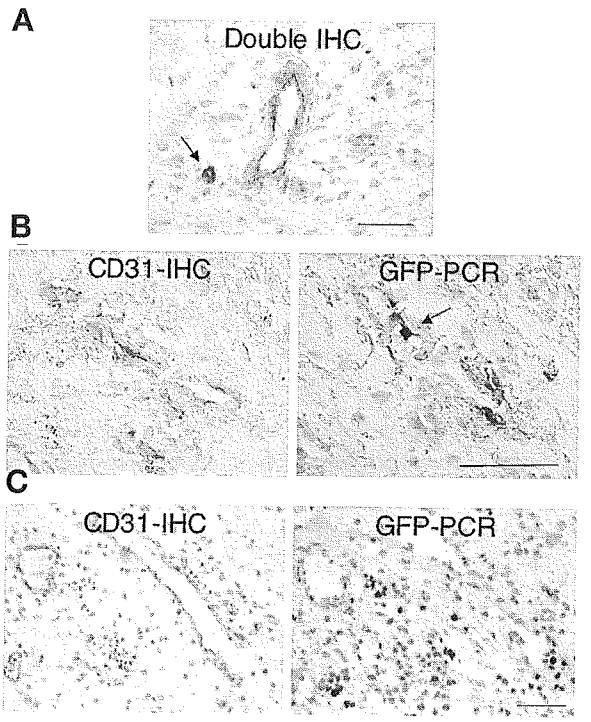

Figure 5. In vivo fate of transplanted cells. Cardiac sections were prepared at 2 weeks after transplantation. **(A)**: Double immunohistochemistry (IHC) with anti-CD31 and anti–green fluorescent protein (GFP) in the peri-infarct region of the CD34$^+$ cell–treated myocardium. Some cells (arrow) were positive for both CD31 (stained in brown) and GFP (stained in black), but such cells were rare. **(B, C)**: Serial sections from the peri-infarct region of the CD34$^+$ cell–treated myocardium. One section (left) was stained with anti-CD31 (stained in brown), and the other (right) was assessed by in situ polymerase chain reaction (PCR) for proviral GFP sequences (stained in black). **(B)**: Some CD31-positive endothelial cells contained the GFP-provirus (arrow, right panel), but such cells were rare. **(C)**: Transplanted cell progeny (cells positive for GFP-provirus in the right panel) were not incorporated in vessels (cells positive for CD31 in the left panel). Bar = 50 μm.

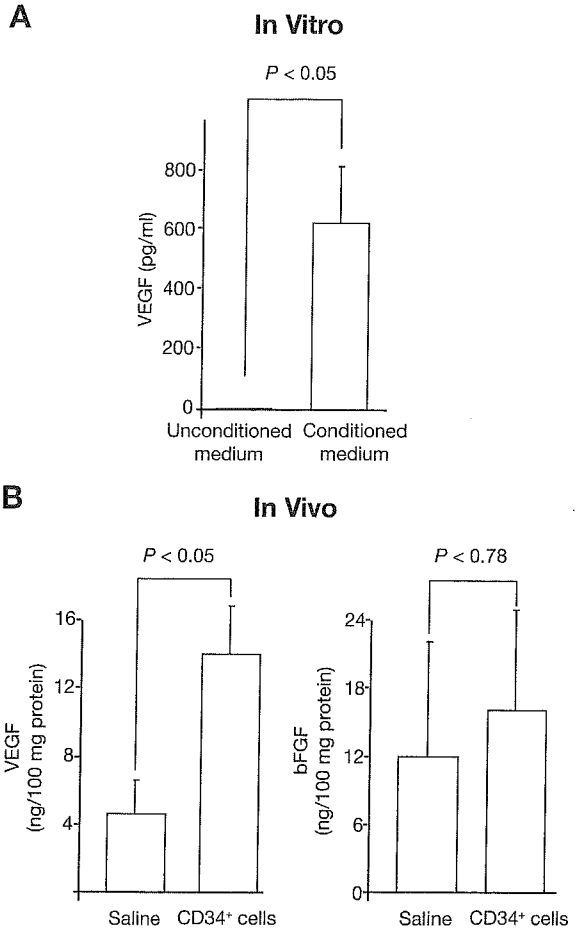

Figure 6. VEGF is implicated in the neoangiogenesis. **(A)**: Unconditioned and conditioned media of in vitro CD34$^+$ cell cultures for endothelial differentiation were examined for VEGF by ELISA. The average ± standard error of six culture dishes is shown. **(B)**: Lysates (three samples per monkey) from the peri-infarct region of the CD34$^+$ cell–treated (monkey, n = 3) and saline-treated (monkey, n = 3) myocardium were prepared and examined for VEGF and basic fibroblast growth factor (bFGF) by ELISA. Data are shown as the average ± standard error. Abbreviation: VEGF, vascular endothelial growth factor.

postentry restriction to HIV-1 infection in simian cells [26]. Unlike HIV-1–based lentiviral vectors, SIV-based ones can efficiently transduce simian hematopoietic stem/progenitor cells [21]. In this study, we also used an SIV-based lentiviral vector and achieved the efficient gene transfer into simian CD34+ cells.

As a result of this marking study, we found only a few GFP-positive cells incorporated into the vascular structure in the ischemic myocardium at 2 weeks after transplantation. GFP-positive cardiomyocytes were not detectable. The existence of GFP-positive endothelial cells can be explained by fusion events [27, 28]. However, if that is the case, GFP-positive cardiomyocytes should have also been detected, given that cardiomyocytes are even easier targets of fusion than endothelial cells [11, 29]. Whether fusion occurred or not, only a few transplanted cells gave rise to nonhematopoietic cells in our primate model.

There are several possible explanations for the very low prevalence of transplanted cell–derived endothelial cells or cardiomyocytes in the ischemic myocardium. First, 2 weeks was too short or the number of transplanted cells was too small to see the nonhematopoietic differentiation. However, the cardiac function and regional blood flow were ameliorated by this time point and with this number of transplanted cells. Thus, if transplanted cell–derived, nonhematopoietic differentiation was a reason for the improvement, transplanted cells at this number should have given rise to such cells by this time point. In fact, Orlic et al. [8] observed transplanted cell-derived endothelial cells and cardiomyocytes within 11 days after transplant in mice. In addition, we observed the endothelial differentiation from CD34+ cells within 7 days in vitro (Fig. 1). However, we cannot formally rule out a possibility that inflammatory responses after generation of infarction might have negative effects on engraftment of transplanted cells. Second, the SIV vector failed to transduce stem or progenitor cells that might be responsible for nonhematopoietic differentiation. Even if the transduction was successful, the cytokine treatment during the transduction or GFP expression in the cells spoiled the differentiation abilities. However, we have shown that the SIV vector successfully transduced cells that were capable of differentiating into GFP-expressing endothelial cells (Fig. 1). We have not examined the differentiation ability to cardiomyocytes, because the method to differentiate CD34+ cells to cardiomyocytes in vitro has not been well established. Thus, we cannot formally rule out the possibility that the ex vivo culture spoiled the ability to differentiate to cardiomyocytes or reduced the ability to differentiate to endothelial cells. Third, cells expressing xenogeneic GFP were rejected via immune responses. However, 2 weeks is too short to allow immune elimination of GFP-expressing cells in monkeys [30, 31]. Fourth, the GFP expression was shut down because of transcriptional silencing in vivo, resulting in negative immunostaining with anti-GFP. To examine this possibility, we tried to detect the provirus (vector integrated into genome) in the cardiac tissue by in situ PCR and found again that only a few CD31-positive endothelial cells contained the GFP-provirus (Fig. 5B), thus arguing against transcriptional silencing-based negative immunostaining with anti-GFP. Taken together, we concluded that most transplanted cell progeny were not incorporated into the repaired, nonhematopoietic tissues.

Our results are in agreement with recent reports that transplanted hematopoietic cells are unable to transdifferentiate into nonhematopoietic cells in ischemic myocardium in mice [9–11]. Our studies confirm and extend these findings in a couple of ways. First, we show that the cardiac function can be indeed significantly improved after injection of hematopoietic cells in a nonhuman primate model, although the above studies used murine myocardial infarction models and did not address the potential beneficial effects of hematopoietic cell injection. Second, the improvement is unlikely to be the result of generation of transplanted cell–derived endothelial cells or cardiomyocytes. Finally, we have found that cultured CD34+ cells secrete VEGF and that the CD34+ cell–treated myocardium contains a significantly higher level of VEGF than the saline-treated myocardium. This observation raises a possibility that some angiogenic cytokines secreted from transplanted cells (paracrine effects) potentiate angiogenic activity of endogenous cells. VEGF would be a candidate. Despite this, the delivery of a single agent (VEGF) failed in clinical trials for cardiac ischemia [32]. In situ multiple cytokine production and coordinated action may be essential for clinical benefits [33, 34]. It will be important to explore and identify cytokines responsible for the paracrine effect. If transplanted cells serve as cytokine factories rather than stem cells in ischemic tissues, it is not surprising that not only stem cells but other types of cells may also work [35]. The concept of stem cell therapeutics for ischemic diseases needs additional consideration.

Acknowledgments

The SIV vector was supplied by DNAVEC Corporation (Ibaraki, Japan), and thrombopoietin was supplied by Kirin Brewery Co. Ltd. (Tokyo). We thank Masahiro Shakudo (Sumiyoshi Hospital, Osaka) for analyzing the contrast echocardiography and Yasuhiro Ochiai (Jichi Medical School) for preparing tissue sections.

References

1 Assmus B, Schachinger V, Teupe C et al. Transplantation of progenitor cells and regeneration enhancement in acute myocardial infarction (TOPCARE-AMI). Circulation 2002;106:3009–3017.

2 Strauer BE, Brehm M, Zeus T et al. Repair of infarcted myocardium by autologous intracoronary mononuclear bone marrow cell transplantation in humans. Circulation 2002;106:1913–1918.

3 Tse HF, Kwong YL, Chan JK et al. Angiogenesis in ischaemic myocardium by intramyocardial autologous bone marrow mononuclear cell implantation. Lancet 2003;361:47–49.

4 Perin EC, Dohmann HF, Borojevic R et al. Transendocardial, autologous bone marrow cell transplantation for severe, chronic ischemic heart failure. Circulation 2003;107:2294–2302.

5 Stamm C, Westphal B, Kleine HD et al. Autologous bone-marrow stem-cell transplantation for myocardial regeneration. Lancet 2003;361:45–46.

6 Wollert KC, Meyer GP, Lotz J et al. Intracoronary autologous bone-marrow cell transfer after myocardial infarction: the BOOST randomised controlled clinical trial. Lancet 2004;364:141-148.

7 Asahara T, Murohara T, Sullivan A et al. Isolation of putative progenitor endothelial cells for angiogenesis. Science 1997;275:964–967.

8 Orlic D, Kajstura J, Chimenti S et al. Bone marrow cells regenerate infarcted myocardium. Nature 2001;410:701–705.

9 Murry CE, Soonpaa MH, Reinecke H et al. Haematopoietic stem cells do not transdifferentiate into cardiac myocytes in myocardial infarcts. Nature 2004;428:664–668.

10 Balsam LB, Wagers AJ, Christensen JL et al. Haematopoietic stem cells adopt mature haematopoietic fates in ischaemic myocardium. Nature 2004;428:668–673.

11 Nygren JM, Jovinge S, Breitbach M et al. Bone marrow-derived hematopoietic cells generate cardiomyocytes at a low frequency through cell fusion, but not transdifferentiation. Nat Med 2004;10:494–501.

12 Hanazono Y, Terao K, Ozawa K. Gene transfer into nonhuman primate hematopoietic stem cells: implications for gene therapy. STEM CELLS 2001;19:12–23.

13 Shibata H, Hanazono Y, Ageyama N et al. Collection and analysis of hematopoietic progenitor cells from cynomolgus macaques (Macaca fascicularis): assessment of cross-reacting monoclonal antibodies. Am J Primatol 2003;61:3–12.

14 Nakajima T, Nakamaru K, Ido E et al. Development of novel simian immunodeficiency virus vectors carrying a dual gene expression system. Hum Gene Ther 2000;11:1863–1874.

15 VandenDriessche T, Thorrez L, Naldini L et al. Lentiviral vectors containing the human immunodeficiency virus type-1 central polypurine tract can efficiently transduce nondividing hepatocytes and antigen-presenting cells in vivo. Blood 2002;100:813–822.

16 Kobayashi N, Yasu T, Yamada S et al. Influence of contrast ultrasonography with perflutren lipid microspheres on microvessel injury. Circ J 2003;67:630–636.

17 Wei K, Jayaweera AR, Firoozan S et al. Quantification of myocardial blood flow with ultrasound-induced destruction of microbubbles administered as a constant venous infusion. Circulation 1998;97:473–483.

18 Hale SL, Alker KJ, Kloner RA. Evaluation of nonradioactive, colored microspheres for measurement of regional myocardial blood flow in dogs. Circulation 1988;78:428–434.

19 Haase AT, Retzel EF, Staskus KA. Amplification and detection of lentiviral DNA inside cells. Proc Natl Acad Sci U S A 1990;87:4971–4975.

20 Hanazono Y, Asano T, Ueda Y et al. Genetic manipulation of primate embryonic and hematopoietic stem cells with simian lentivirus vectors. Trends Cardiovasc Med 2003;13:106–110.

21 Hanawa H, Hematti P, Keyvanfar K et al. Efficient gene transfer into rhesus repopulating hematopoietic stem cells using a simian immunodeficiency virus-based lentiviral vector system. Blood 2004;103:4062–4069.

22 Miyoshi H, Smith KA, Mosier DE et al. Transduction of human $CD34^+$ cells that mediate long-term engraftment of NOD/SCID mice by HIV vectors. Science 1999;283:682–686.

23 Horn PA, Keyser KA, Peterson LJ et al. Efficient lentiviral gene transfer to canine repopulating cells using an overnight transduction protocol. Blood 2004;103:3710–3716.

24 Dunbar CE, Takatoku M, Donahue RE. The impact of ex vivo cytokine stimulation on engraftment of primitive hematopoietic cells in a non-human primate model. Ann N Y Acad Sci 2001;938:236–245.

25 Owens CM, Yang PC, Gottlinger H et al. Human and simian immunodeficiency virus capsid proteins are major viral determinants of early, postentry replication blocks in simian cells. J Virol 2003;77:726–731.

26 Stremlau M, Owens CM, Perron MJ et al. The cytoplasmic body component TRIM5α restricts HIV-1 infection in Old World monkeys. Nature 2004;427:848–853.

27 Terada N, Hamazaki T, Oka M et al. Bone marrow cells adopt the phenotype of other cells by spontaneous cell fusion. Nature 2002;416:542–545.

28 Ying QL, Nichols J, Evans EP et al. Changing potency by spontaneous fusion. Nature 2002;416:545–548.

29 Alvarez-Dolado M, Pardal R, Garcia-Verdugo JM et al. Fusion of bone-marrow-derived cells with Purkinje neurons, cardiomyocytes and hepatocytes. Nature 2003;425:968–973.

30 Rosenzweig M, Connole M, Glickman R et al. Induction of cytotoxic T lymphocyte and antibody responses to

enhanced green fluorescent protein following transplantation of transduced CD34(+) hematopoietic cells. Blood 2001;97:1951–1959.

31 Heim DA, Hanazono Y, Giri N et al. Introduction of a xenogeneic gene via hematopoietic stem cells leads to specific tolerance in a rhesus monkey model. Mol Ther 2000;1:533–544.

32 Henry TD, Annex BH, McKendall GR et al. The VIVA trial: vascular endothelial growth factor in ischemia for vascular angiogenesis. Circulation 2003;107:1359–1365.

33 Cao R, Brakenhielm E, Pawliuk R et al. Angiogenic synergism, vascular stability and improvement of hind-limb ischemia by a combination of PDGF-BB and FGF-2. Nat Med 2003;9:604–613.

34 Ziegelhoeffer T, Fernandez B, Kostin S et al. Bone marrow-derived cells do not incorporate into the adult growing vasculature. Circ Res 2004;94:230–238.

35 Kinnaird T, Stabile E, Burnett MS et al. Local delivery of marrow-derived stromal cells augments collateral perfusion through paracrine mechanisms. Circulation 2004;109:1543–1549.

Gene Therapy (2005) 12, 203–210

www.nature.com/gt

RESEARCH ARTICLE

Efficient and stable Sendai virus-mediated gene transfer into primate embryonic stem cells with pluripotency preserved

K Sasaki[1,2], M Inoue[3], H Shibata[1], Y Ueda[3], S-i Muramatsu[4], T Okada[1], M Hasegawa[3], K Ozawa[1] and Y Hanazono[1]

[1]*Center for Molecular Medicine, Jichi Medical School, Minamikawachi, Tochigi, Japan;* [2]*Department of Plastic and Reconstructive Surgery, Faculty of Medicine, University of Tokyo, Bunkyo-ku, Tokyo, Japan;* [3]*DNAVEC Corporation, Tsukuba, Ibaraki, Japan; and* [4]*Department of Neurology, Jichi Medical School, Minamikawachi, Tochigi, Japan*

Efficient gene transfer and regulated transgene expression in primate embryonic stem (ES) cells are highly desirable for future applications of the cells. In the present study, we have examined using the nonintegrating Sendai virus (SeV) vector to introduce the green fluorescent protein (GFP) gene into non-human primate cynomolgus ES cells. The GFP gene was vigorously and stably expressed in the cynomolgus ES cells for a year. The cells were able to form fluorescent teratomas when transplanted into immunodeficient mice. They were also able to differentiate into fluorescent embryoid bodies, neurons, and mature blood cells. In addition, the GFP expression levels were reduced dose-dependently by the addition of an anti-RNA virus drug, ribavirin, to the culture. Thus, SeV vector will be a useful tool for efficient gene transfer into primate ES cells and the method of using antiviral drugs should allow further investigation for regulated SeV-mediated gene expression.
Gene Therapy (2005) **12,** 203–210. doi:10.1038/sj.gt.3302409
Published online 14 October 2004

Keywords: *primate embryonic stem cell; Sendai virus vector; gene transfer; green fluorescent protein; pluripotency; ribavirin*

Introduction

Since human embryonic stem (ES) cell lines have the ability to both proliferate indefinitely and differentiate into multiple tissue cells,[1,2] they are expected to have clinical applications as well as to serve as models for basic research and drug development. Although efficient and stable gene transfer into primate ES cells would be useful for such purposes, it has been difficult and only lentiviral vectors have been successful in achieving it.[3–5] We have previously developed Sendai virus (SeV) vectors that replicate in the form of negative-sense single-stranded RNA in the cytoplasm of infected cells and do not go through a DNA phase.[6] SeV vectors can efficiently introduce foreign genes without toxicity into airway epithelial cells,[7] vascular tissue,[8] skeletal muscle,[9] synovial cells,[10] retinal tissue,[11] and hematopoietic progenitor cells.[12] Here we report that the SeV-mediated gene transfer into primate ES cells is very efficient and stable even after the terminal differentiation of the cells. In addition, we show that SeV-mediated transgene expression levels can be reduced by the addition of a ribonucleoside analog, ribavirin, to the culture. Ribavirin is a mutagen and inhibitor of viral RNA polymerase.[13,14] It shows antiviral activity against a variety of RNA viruses and is used to treat infections of hepatitis C virus in combination with interferon-α[15,16] and of lassa fever virus.[17] The method of using antiviral drugs might offer a novel approach for regulated SeV-mediated gene expression in primate ES cells.

Correspondence: Dr Y Hanazono, Center for Molecular Medicine, Jichi Medical School, 3311-1 Yakushiji, Minamikawachi, Tochigi 329-0498, Japan
Received 20 April 2004; accepted 27 August 2004; published online 14 October 2004

Results

SeV-mediated gene transfer into ES cells

In this study, we have used an SeV vector, which is capable of self-replication but incapable of transmitting to other cells.[6] The vector does not encode the fusion (F) protein (Figure 1a), which is essential for viral entry into cells. It can be propagated only in a packaging cell line expressing the F protein. The green fluorescent protein (GFP) gene was introduced after the leader sequence of the vector genome. Cynomolgus ES cells[18] were exposed to the SeV vector for 24 h. Flow cytometric analysis at 2 days after infection showed that 15, 38, and 61% of cells fluoresced at 2, 10, and 50 transducing units (TU) per cell, respectively (Figure 1b). The gene transfer efficiency of about 60% is comparable to or even better than that for lentiviral vectors.[3] We confirmed that the undifferentiated cell fractions remained unchanged after the infection with SeV vector, as assessed by the expression of undifferentiated markers, alkaline phosphatase and SSEA-4 (data not shown). The GFP expression after infection was stable at least for a month. On the other hand, the GFP gene transfer to cynomolgus ES cells with adenovirus- and adeno-associated virus (AAV)-based vectors resulted in much lower expression levels (<20% by flow cytometry) and the levels declined to zero within a week after infection (Figure 1c).

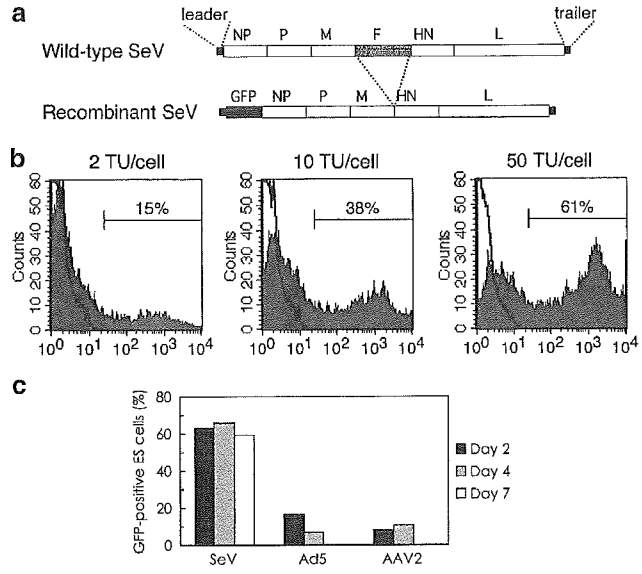

Figure 1 High-level transgene expression in cynomolgus ES cells after infection with SeV vector. (a) Schematic diagrams of the wild-type SeV genome and recombinant F-defective SeV carrying the GFP gene (SeV vector in this study). The SeV genome is 15 384 nucleotides long and its genes (NP, P, M, F, HN, and L) are in order from 3′ to 5′ in the negative-strand RNA. In the SeV vector, the entire fusion (F) gene was removed and the GFP gene was introduced at a unique NotI site between the leader sequence and NP gene. (b) The GFP expression by the SeV vector in cynomolgus ES cells. Cynomolgus ES cells were infected with the SeV vector at 2, 10, and 50 TU/cell. The flow cytometric profiles at day-2 postinfection are shown in gray. The white areas indicate uninfected ES cells. The fractions of GFP-positive cells are indicated. (c) The GFP expression levels in cynomolgus ES cells infected with the SeV (50 TU/cell), adenovirus serotype 5 (Ad5, 3.4×10^2 g.c./cell), and AAV serotype 2 (AAV2, 2.4×10^4 g.c./cell) vectors. The fractions of GFP-positive cells were examined by flow cytometry at 2, 4, and 7 days postinfection.

We plucked fluorescent ES cell colonies under a fluorescent microscope once at 1 month after infection and propagated them. After this selection procedure, approximately 90% of the ES cells expressed GFP (Figure 2a and b) and the high-level expression was stable for a year as assessed by flow cytometry (Figure 2c, upper). The mean fluorescence intensity per cell was also stable (Figure 2c, lower), indicating that the replicating vector genome was almost equally delivered to each cell of all progeny. The self-replication of the SeV vector in infected cells was confirmed by RNA-PCR that amplified the viral RNA genomic sequence (Figure 3a). The GFP cDNA sequence, however, could not be detected by DNA-PCR in the infected cells (Figure 3b), indicating that no DNA phase was involved in the GFP expression.

Pluripotency of infected ES cells

The SeV-infected, fluorescent cynomolgus ES cells were able to form fluorescent tumors when transplanted into immunodeficient mice (Figure 4a–c). The fluorescence was observed uniformly by fluorescent microcopy (Figure 4d and e). The tumors consisted of all three embryonic germ layer cells (Figure 4f–i). Thus, the SeV-infected ES cells were capable of forming teratomas and the SeV infection did not spoil the pluripotency of ES cells. The infected, fluorescent cynomolgus ES cells were also able to generate fluorescent embryoid bodies (Figure 5a and b), MAP-2-positive neurons (Figure 5c), clonogenic hematopoietic colonies (Figure 5d and e), and mature functional (NBT test-positive) neutrophils (Figure 5f and g), all of which fluoresced. In addition, the GFP expression levels were not decreased during the teratoma formation or differentiation, indicating that no 'silencing' of the transgene occurred.

Drug-inducible reduction of transgene expression

Next, we examined whether ribavirin inhibits the replication and transcription of the SeV vector resulting in a reduction of transgene expression. We first used a rhesus monkey kidney cell line (LLC-MK2) to test the effect of ribavirin on the replication and transcription of the SeV vector. LLC-MK2 is a standard control cell line for SeV infection. Ribavirin was added at various concentrations 2 days after the infection. The formation of viral particles quantified by the hemagglutination assay decreased drastically upon the addition of ribavirin (Figure 6a). The decrease was dependent on the dose of ribavirin. The GFP expression was also depressed dose-dependently (Figure 6b). Thus, ribavirin dose-dependently inhibits the replication and transcription of the SeV vector in LLC-MK2 cells. The toxicity associated with ribavirin was not observed in LLC-MK2 cells.

We then examined the effect of ribavirin on SeV-infected, fluorescent cynomolgus ES cells. The addition of ribavirin also resulted in a dose-dependent reduction of GFP expression in the cells (Figure 6c). Although the GFP expression was almost completely inhibited after a 3-day exposure with 4 mM of ribavirin, the cells could not be propagated thereafter. Ribavirin at high concentrations (>1 mM) hampered the proliferation of cynomolgus ES cells. With lower concentrations (0.5–0.75 mM) of ribavirin, the GFP expression level decreased by half. After the discontinuation of ribavirin treatment, the cells could be propagated and nearly regained the original level of GFP expression. The undifferentiated cell fractions were unchanged after the discontinuation as assessed by alkaline phosphatase and SSEA-4 staining (Figure 6d).

Discussion

There are several advantages in using SeV vectors over other vectors. (i) SeV vectors can infect nondividing, quiescent cells as well as dividing cells unlike oncoretroviral vectors.[7–11] Thus, they can be used to infect cells that are terminally differentiated as well as at various stages of differentiation, whether they are dividing or not. (ii) SeV vector-mediated gene transfer does not require a DNA phase. Thus, there is no concern about the unwanted integration of foreign sequences into the host genome unlike with oncoretroviral or lentiviral vectors. (iii) Transgene expression is stable even in dividing cells since the SeV vector replicates by itself in the cytoplasm of host cells. On the other hand, gene transfer using nonreplicating adenoviral and AAV vectors resulted in decreased levels of transgene expression in dividing cells over time, since the non-replicating transgene was

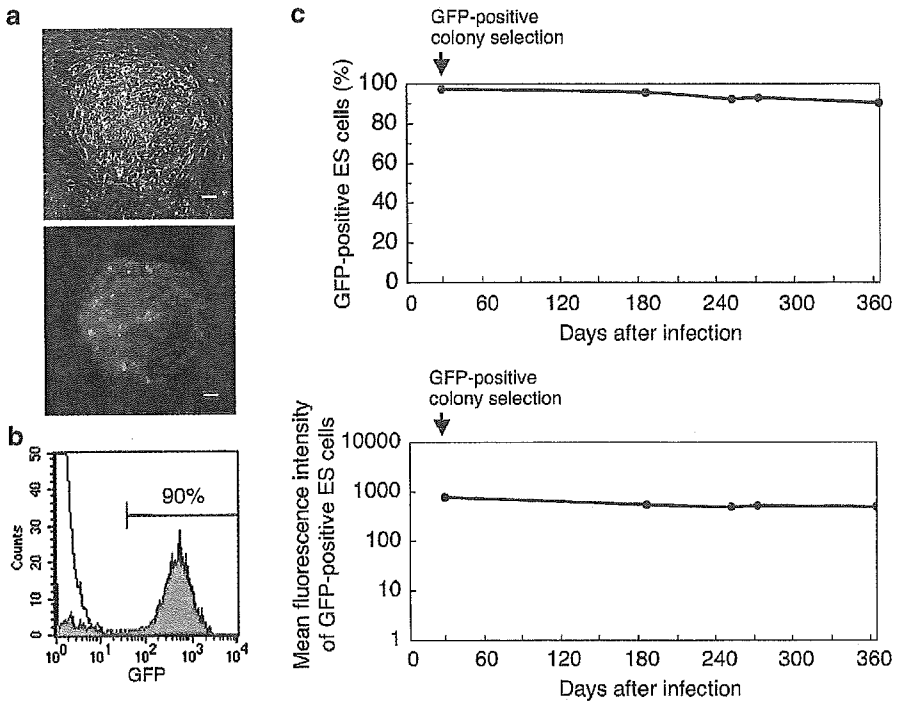

Figure 2 Stable SeV-mediated transgene expression in cynomolgus ES cells. Fluorescent ES cell colonies were plucked under a fluorescent microscope once at 1 month after infection and the cells were further propagated. (a) Phase-contrast (upper) and fluorescence (lower) images of a cynomolgus ES cell colony at day 370 after infection. Bar = 100 μm. (b) Flow cytometric analysis of SeV-infected cynomolgus ES cells at day 370 after infection (shown in green). The percentage of GFP-positive cells is indicated. Uninfected, parental cynomolgus ES cells are indicated by another line (white area). (c) The percentage of GFP-positive cells (upper) and mean fluorescence intensity per GFP-positive cell (lower) after infection with the SeV vector at 10 TU/cell are shown as a function of time (days).

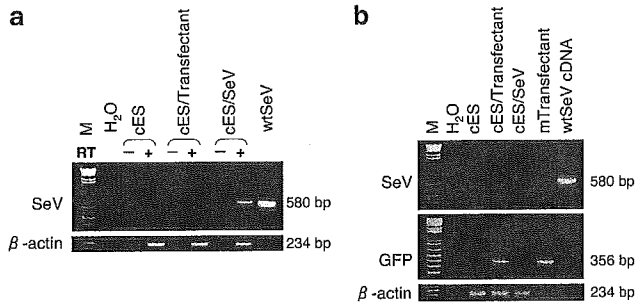

Figure 3 DNA-independent replication and transcription of SeV vector. Total cellular RNA and DNA were extracted from cynomolgus ES cells at day 284 after infection with the SeV vector. RNA-PCR (a) and DNA-PCR (b) for the SeV RNA genome or GFP sequence were conducted. The cynomolgus β-actin sequence was used as an internal control. In the RNA-PCR (a), negative results obtained without reverse transcriptase (designated RT−) confirmed that the amplified products were not derived from cellular DNA. M, 100-kb DNA ladder; cES, naive cynomolgus ES cells; cES/Transfectant, cynomolgus ES cells stably expressing the GFP gene after transfection,[33] cES/SeV, cynomolgus ES cells infected with the SeV vector; wtSeV, wild-type SeV genome; mTransfectant, a GFP-positive mouse cell line after transfection.

diluted out. (iv) The SeV vector is much less unlikely to generate wild-type virus *in vitro* or *in vivo* than oncoretroviral and lentiviral vectors, since homologous recombination between RNA genomes is very rare indeed in negative-strand RNA viruses.[19] (v) The SeV genome is not subject to cellular epigenetic modifications such as methylation, and thus it is unlikely that methylation-based silencing of transgene expression occurs.

No cytotoxic or differentiating effect on ES cells associated with the SeV infection was observed in our study. However, the wild-type SeV contains immunogenic surface proteins, hemagglutinin-neuraminidase (HN) and F proteins, which potentially induce antibody responses.[20,21] For future clinical applications, it would be desired that as many viral genes as possible are deleted from the vector backbone to permit reapplication, improve the safety, and lessen the possible toxicity of SeV vectors. To this end, we have developed a series of attenuated SeV vectors that are F gene-deleted,[6] F gene-deleted with preferable mutations,[22] M gene-deleted,[23] or have deletions of both F and M genes.[24] The modified vectors would be safer for *in vivo* use.

Ribavirin at high concentrations seems toxic to ES cells; presumably, it directly hampers viability and proliferation potential of ES cells. However, we cannot tell whether the observed toxicity is simply due to its toxicity to ES cells, as feeder cells are more highly sensitive to ribavirin than ES cells. In fact, while feeder cells died at 1 mM of ribavirin, cocultured ES cells were alive at this concentration for some time. Cynomolgus ES cells lose pluripotency and proliferation potential without feeder cells. Thus, the observed toxicity to ES cells may also be a secondary event following the injury of feeder cells. Whether the cytotoxicity is primary or secondary, it will be necessary to find modified compounds of less cytotoxicity.

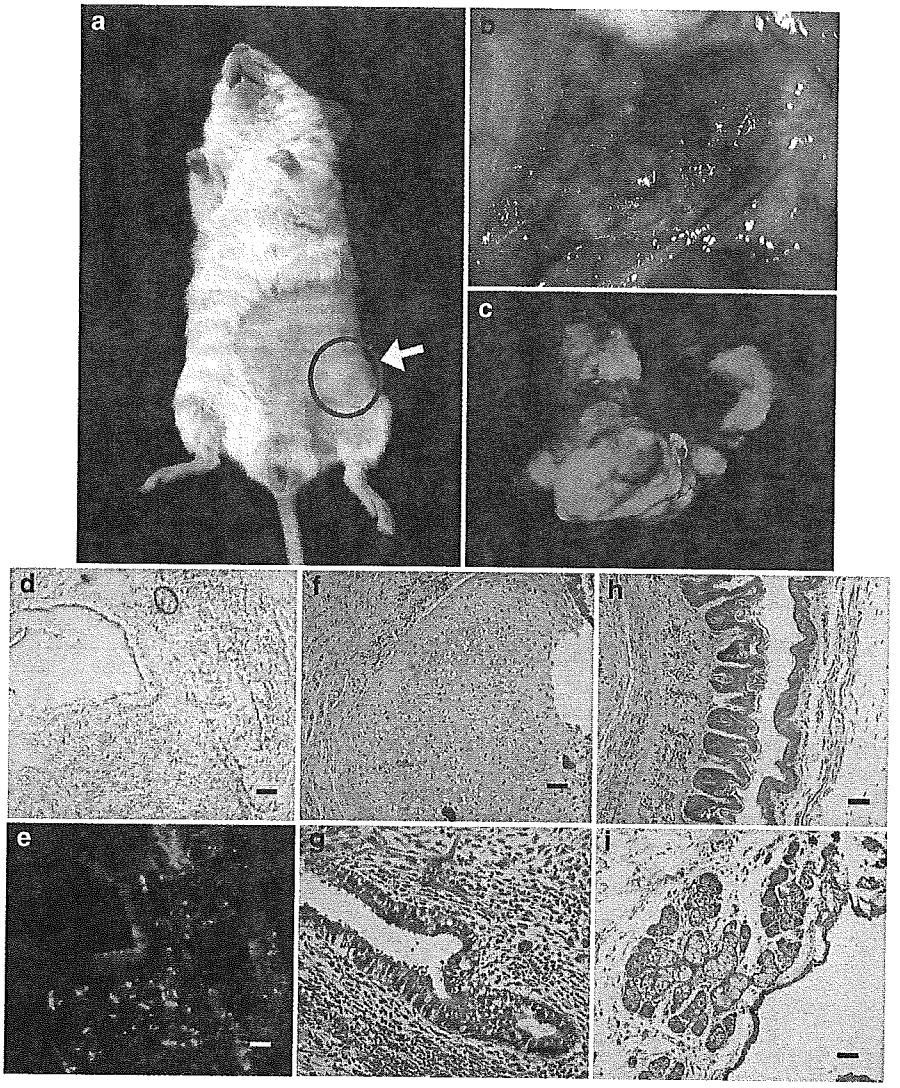

Figure 4 Pluripotency of SeV-infected cynomlgus ES cells. Tumors formed in NOD-SCID mice after inoculation of the SeV-infected cynomolgus ES cells (a). The tumor was fluorescing ((b), bright field; (c), dark field). Fluorescence was observed uniformly in the tumor under a fluorescent microscope ((d), bright field; (e), dark field). The tumor contained all three embryonic germ layer cells; cartilage (f), ciliated columnar epithelium (g), skin (h), and sebaceous gland (i) (stained with hematoxylin and eosin). Bar = 100 μm.

Materials and methods

Cell culture

Cynomolgus ES cells (CMK6) were maintained on a feeder layer of mitomycin C (Kyowa, Tokyo, Japan)-treated mouse (BALB/c) embryonic fibroblasts as described previously.[18] The culture medium consisted of Dulbecco's modified Eagle's medium (DMEM)/F12 (Invitrogen, Carlsbad, CA, USA) supplemented with 15% ES cell-qualified fetal calf serum (FCS; Invitrogen), 0.1 mM 2-mercaptoethanol (Sigma, St Louis, MO, USA), 2 mM glutamine (Invitrogen), 0.1 mM nonessential amino acids (Invitrogen), and antibiotics (100 U/ml penicillin and 100 μg/ml streptomycin, Irvine Scientific, Santa Ana, CA, USA). The ES cell colonies were routinely passaged every 3–4 days after dissociation with a combined approach of 0.25% trypsin (Invitrogen) digestion and mechanical cutting. Alkaline phosphatase staining was conducted with an Alkaline Phosphatase Chromogen Kit (Biomeda, Foster City, CA, USA). Embryoid bodies were produced by culturing ES cell aggregates in Petri dishes. LLC-MK2 cells (1×10^6) were grown in six-well plates and cultured in Eagle's minimal essential medium (Invitrogen) supplemented with 10% FCS.

Vectors

The F-defective SeV vector carrying the GFP gene was constructed as previously described.[6] The vector titer was 1.8×10^9 TU/ml determined by counting fluorescent cells after the infection of LLC-MK2 cells. Gene transfer was conducted by adding various concentrations of the SeV vector solution to culture media. After 24 h of incubation, the cells were washed twice with phosphate-buffered saline (PBS) and fresh medium was added. In some experiments, ribavirin (1-β-D-ribofuranosyl-1,2,4-triazole-3-carboxamide; Sigma) was added at various concentrations to the culture media after infection. The

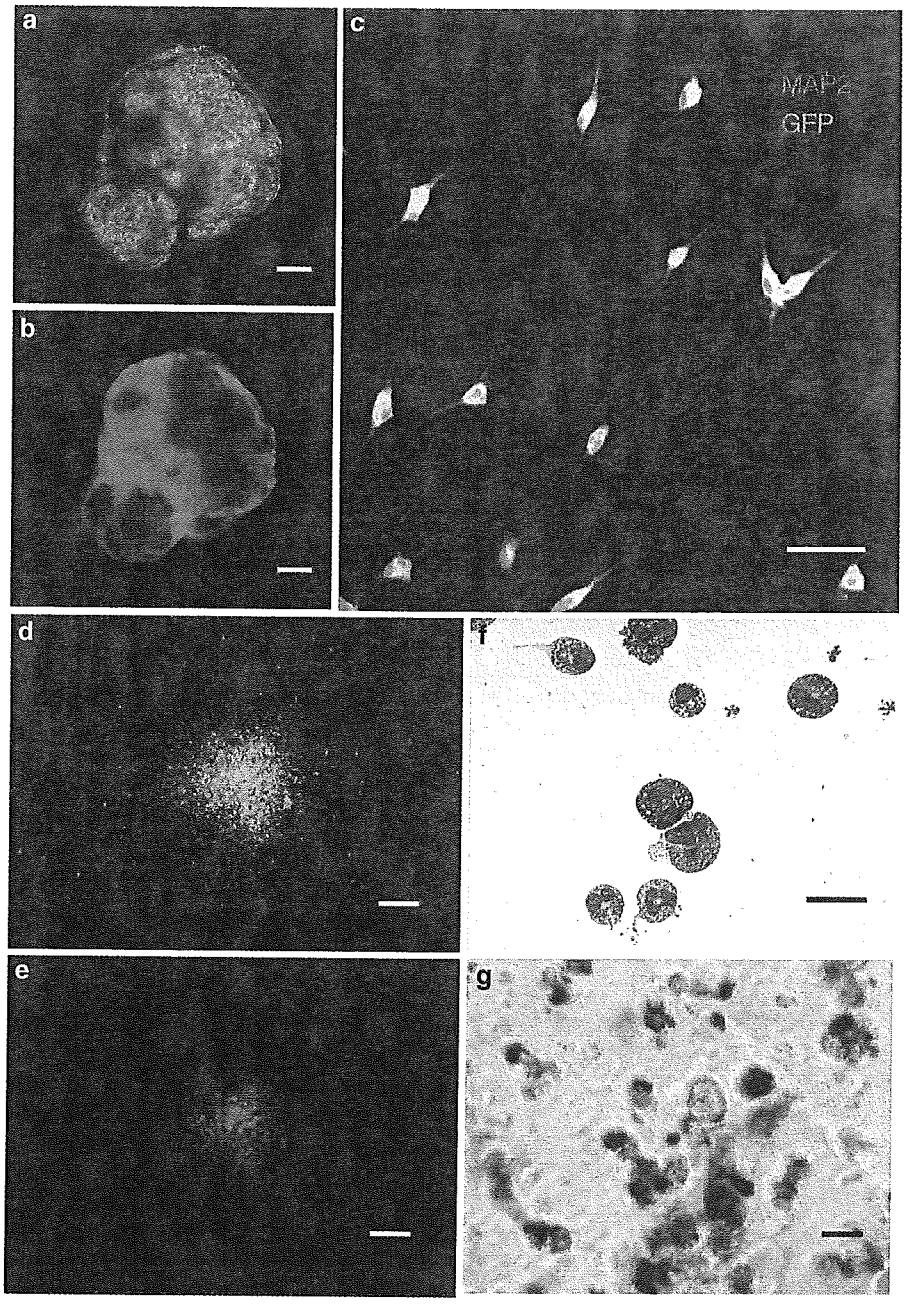

Figure 5 *Stable transgene expression during differentiation. A day-20 cystic embryoid body was observed under a fluorescent phase-contrast microscope, confirming that the embryoid body was fluorescing ((a), bright field; (b), dark field). After infection with the SeV vector, fluorescent cynomolgus ES cells differentiated into neural cells. Double immunostaining with anti-GFP (green) and ant-MAP-2 (red) confirmed that differentiated neural cells expressed GFP (c). Yellow cells indicate GFP-expressing neurons. SeV-infected, fluorescent cynomolgus ES cells also differentiated into fluorescent hematopoietic cells. A clonogenic hematopoietic colony was fluorescing ((d) bright field; (e), dark field). A cytospin specimen of hematopoietic colony cells (Wright–Giemsa staining) showed that the cells were mature granulocytes (f). The infected ES cell-derived, fluorescent neutrophils were positive for NBT (stained in black (g)). Bar = 100 μm (a, b, g); 50 μm (c, f); 500 μm (d, e).*

viral particles in infected cells were quantified by a hemagglutination assay as described previously.[25]

An adenovirus serotype 5-based vector carrying the GFP gene was constructed as reported.[26] It contained the cytomegalovirus (CMV) promoter, simian virus (SV)-40 intron, and SV-40 polyadenylation signal. An AAV serotype 2-based vector expressing the GFP gene under the control of the chicken β-actin promoter with the CMV immediate-early enhancer (a gift from Dr J Miyazaki) was prepared as described previously.[27] Gene transfer experiments were performed using 3.4×10^2 genome copies (g.c.)/cell of the adenoviral vector or 2.4×10^4 g.c./cell of the AAV vector. The period of exposure was 48 h.

Flow cytometry

GFP and SSEA-4 expression was analyzed on a FACScan (Becton Dickinson, Franklin Lakes, NJ, USA) using the

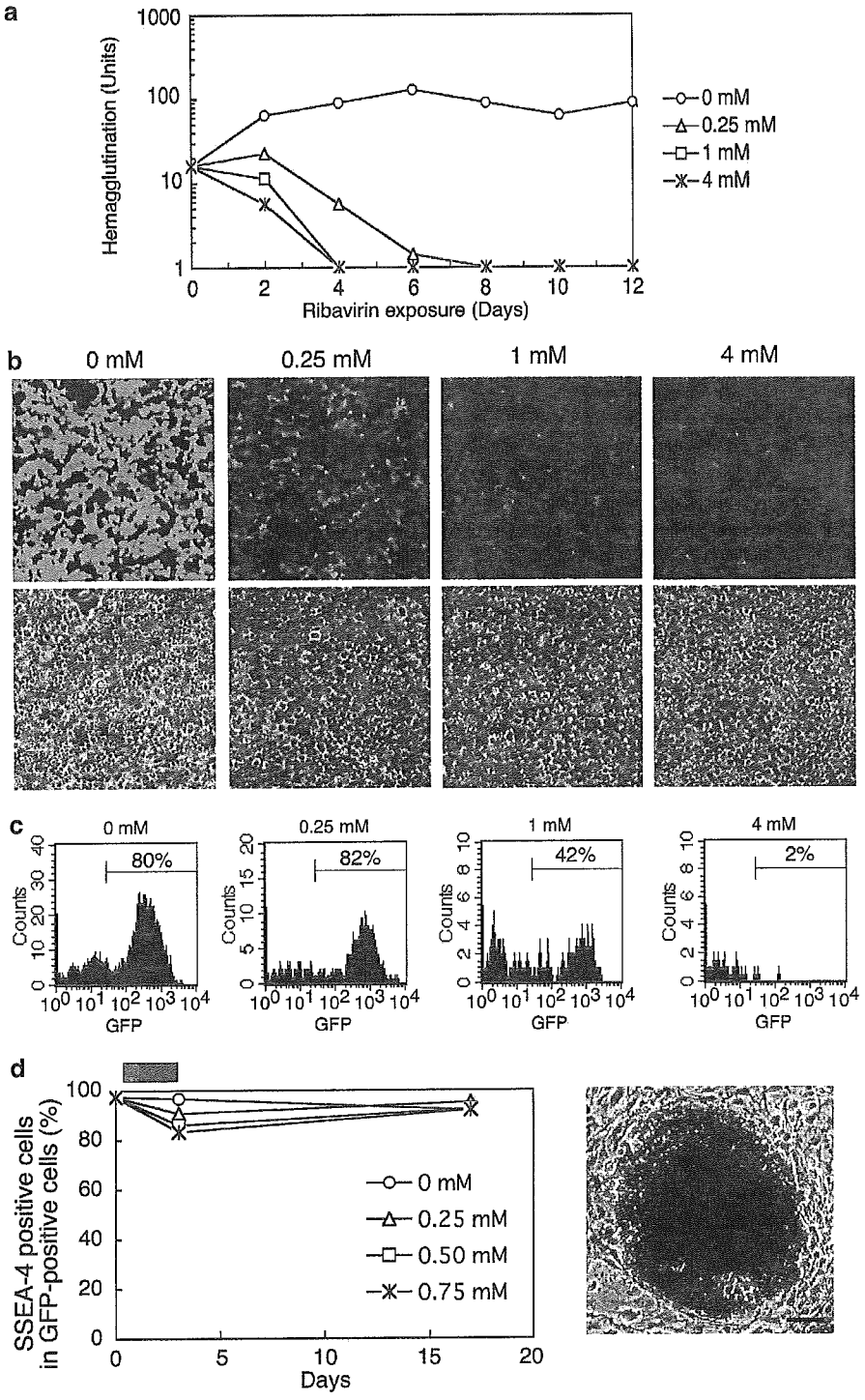

Figure 6 *Ribavirin-regulated transgene expression. (a) A rhesus kidney cell line (LLC-MK2) was infected with the SeV vector at 3 TU/cell. Ribavirin was started at various concentrations on day 2 after the infection. The formation of viral particles in the infected LLC-MK2 cells was examined by the hemagglutination assay. (b) The ribavirin-treated LLC-MK2 cells were observed under a fluorescent microscope after an 8-day exposure of ribavirin (upper, dark field; lower, bright field). (c) Ribavirin was added at various concentrations to the SeV-infected, fluorescent cynomolgus ES cells. The GFP expression was assessed by flow cytometry after a 3-day exposure of ribavirin. (d) The fractions of SSEA-4-positive ES cells were assessed by flow cytometry with anti-SSEA-4 before and after a 3-day exposure of ribavirin and are shown as a function of time (days) in the left panel. A gray bar indicates ribavirin treatment. ES cells were stained for alkaline phosphatase (in red) at day 21 after a 3-day exposure of 0.75 mM ribavirin and are shown in the right panel. Bar = 100 μm.*

CellQuest software (Becton Dickinson). For SSEA-4 staining, cells were incubated with a primary antibody, anti-SSEA-4 (MC-813-70; Chemicon, Temecula, CA, USA), and then a secondary antibody, PE-conjugated F(ab')2 fragment of rabbit anti-mouse immunoglobulins (DakoCytomation, Glostrup, Denmark). Cocultured BALB/c feeder cells could be distinguished from cynomolgus ES cells by using PE-conjugated anti-mouse

H-2d (SF1-1.1; PharMingen, San Diego, CA, USA), which does not react to cynomolgus cells but does react to BALB/c cells.

Teratoma formation

Cynomolgus ES cells (approximately 10^6 cells per site) were injected subcutaneously into the hind leg of 6- to 8-week-old nonobese diabetic/severe combined immunodeficient mice (Jackson Laboratory, Bar Harbor, ME, USA). The resulting tumors (usually 9–12 weeks after the injection) were dissected and fixed in 4% paraformaldehyde. For histological analysis, samples from the tumors were embedded in paraffin and stained with hematoxylin and eosin. To observe GFP fluorescence, samples were embedded in OTC compound (Sakura, Zoeterwoude, Netherlands), frozen, sectioned, and examined under a fluorescence microscope.

Hematopoietic differentiation

The mouse bone marrow stromal cell line OP9 was maintained in α-modified minimum essential medium (Invitrogen) supplemented with 20% FCS as described previously.[28] For induction of hematopoietic differentiation, ES cells were seeded onto a mitomycin C-treated confluent OP9 cell layer in six-well plates. Medium to support the differentiation was described elsewhere.[29] Cells at day 18 were placed in Methocult GF+ media (StemCell Technologies, Vancouver, Canada) at 1×10^4 and 1×10^5 cells per plate and clonogenic hematopoietic colonies were produced. After 14 days, individual colonies were removed and spun onto glass slides. Cells were stained with the Wright–Giemsa method. The nitro blue tetrazolium (NBT, Sigma) reduction test was performed on the cells as a granulocyte functional assay according to a previously described method.[30]

Neural differentiation

The induction of neural differentiation was carried out as described previously.[31] Day-4 embryoid bodies were plated onto tissue culture dishes and nestin-positive cells were selected in DMEM/F12 medium supplemented with 5 μg/ml of insulin (Sigma), 50 μg/ml of transferrin (Sigma), 30 nM selenium chloride (Sigma), and 5 μg/ml of fibronectin (Sigma) for 5 days. Cells were then trypsinized and plated in polyornithine-coated dishes (15 μg/ml) and expanded in N2 medium[32] supplemented with 1 μg/ml of laminin (Sigma) and 10 μg/ml of basic fibroblast growth factor (bFGF; Roche, Basel, Switzerland) for 6 days. Differentiation was induced by removal of bFGF. To confirm the neural differentiation, cells were stained with anti-human MAP-2. Briefly, cells were fixed in 4% paraformaldehyde in PBS and incubated with anti-human MAP-2 (HM-2; Sigma; diluted 1:4000) and then by Alexa Fluor 594-labeled antibody (diluted 1:500; Molecular Probe, Eugene, OR, USA). The samples were examined under a fluorescence microscope.

DNA-PCR

DNA-PCR for the SeV genome and GFP sequences was carried out as follows. DNA was extracted using the QIAamp DNA mini kits (Qiagen, Hilden, Germany) and 250 ng was used for each PCR with ExTaq (Takara, Shiga, Japan). Amplification conditions were 30 cycles of 94°C for 1 min, a variable annealing temperature (noted below) for 1 min, and 72°C for 1 min. The amplified products were run on 2% agarose gel and visualized by ethidium bromide staining. Primer sequences, annealing temperatures and product sizes were as follows: the SeV vector genome sequence: 5′-AGA GAA CAA GAC TAA GGC TAC C-3′ and 5′-ACC TTG ACA ATC CTG ATG TGG-3′ (55°C, 580 bp); the GFP sequence: 5′-CGT CCA GGA GCG CAC CAT CTT C-3′ and 5′-GGT CTT TGC TCA GGG CGG ACT-3′ (60°C, 356 bp). the cynomolgus β-actin sequence: 5′-CAT TGT CAT GGA CTC TGG CGA CGG-3′ and 5′-CAT CTC CTG CTC GAA GTC TAG GGC-3′ (60°C, 234 bp).

RNA-PCR

RNA-PCR for the SeV RNA genomic sequence was carried out as follows. Total RNA was extracted using RNA STAT-60 (Tel-Test, Friendswood, TX, USA). Reverse transcription was conducted by using Taqman reverse transcription reagents (Applied Biosystems, Foster City, CA, USA). The product (250 ng) after the reverse transcription was used for the subsequent PCR as described above.

Acknowledgements

Cynomolgus ES cells were provided by Norio Nakatsuji (Kyoto University, Kyoto, Japan), Yasushi Kondo (Tanabe Seiyaku Co. Ltd, Osaka, Japan), and Ryuzo Torii (Shiga University of Medical Science, Shiga, Japan). OP9 cells were provided by Toru Nakano (Osaka University, Osaka, Japan). We thank Yujiro Tanaka and Takayuki Asano for cultivating cynomolgus ES cells and Takeshi Hara for conducting NBT tests. We also thank Natsuko Kurosawa for technical assistance.

References

1 Thomson JA *et al.* Embryonic stem cell lines derived from human blastocysts. *Science* 1998; **282**: 1145–1147.
2 Reubinoff BE *et al.* Embryonic stem cell lines from human blastocysts: somatic differentiation *in vitro*. *Nat Biotechnol* 2000; **18**: 399–404.
3 Asano T *et al.* Highly Efficient gene transfer into primate embryonic stem cells with a simian lentivirus vector. *Mol Ther* 2002; **6**: 162–168.
4 Ma Y *et al.* High-level sustained transgene expression in human embryonic stem cells using lentiviral vectors. *Stem Cells* 2003; **21**: 111–117.
5 Gropp M *et al.* Stable genetic modification of human embryonic stem cells by lentiviral vectors. *Mol Ther* 2003; **7**: 281–287.
6 Li HO *et al.* A cytoplasmic RNA vector derived from nontransmissible Sendai virus with efficient gene transfer and expression. *J Virol* 2000; **74**: 6564–6569.
7 Yonemitsu Y *et al.* Efficient gene transfer to airway epithelium using recombinant Sendai virus. *Nat Biotechnol* 2000; **18**: 970–973.
8 Masaki I *et al.* Recombinant Sendai virus-mediated gene transfer to vasculature: a new class of efficient gene transfer vector to the vascular system. *FASEB J* 2001; **15**: 1294–1296.
9 Shiotani A *et al.* Skeletal muscle regeneration after insulin-like growth factor I gene transfer by recombinant Sendai virus vector. *Gene Therapy* 2001; **8**: 1043–1050.
10 Yamashita A *et al.* Fibroblast growth factor-2 determines severity of joint disease in adjuvant-induced arthritis in rats. *J Immunol* 2002; **168**: 450–457.

11 Ikeda Y *et al.* Recombinant Sendai virus-mediated gene transfer into adult rat retinal tissue: efficient gene transfer by brief exposure. *Exp Eye Res* 2002; **75**: 39–48.
12 Jin CH *et al.* Recombinant Sendai virus provides a highly efficient gene transfer into human cord blood-derived hematopoietic stem cells. *Gene Therapy* 2003; **10**: 272–277.
13 Crotty S *et al.* The broad-spectrum antiviral ribonucleoside ribavirin is an RNA virus mutagen. *Nat Med* 2000; **6**: 1375–1379.
14 Vo NV, Young KC, Lai MM. Mutagenic and inhibitory effects of ribavirin on hepatitis C virus RNA polymerase. *Biochemistry* 2003; **42**: 10462–10471.
15 McHutchison JG *et al.* Interferon alfa-2b alone or in combination with ribavirin as initial treatment for chronic hepatitis C. Hepatitis Interventional Therapy Group. *N Engl J Med* 1998; **339**: 1485–1492.
16 Davis GL *et al.* Interferon alfa-2b alone or in combination with ribavirin for the treatment of relapse of chronic hepatitis C. International Hepatitis Interventional Therapy Group. *N Engl J Med* 1998; **339**: 1493–1499.
17 McCormick JB *et al.* Lassa fever. Effective therapy with ribavirin. *N Engl J Med* 1986; **314**: 20–26.
18 Suemori H *et al.* Establishment of embryonic stem cell lines from cynomolgus monkey blastocysts produced by IVF or ICSI. *Dev Dyn* 2001; **222**: 273–279.
19 Spann KM, Collins PL, Teng MN. Genetic recombination during coinfection of two mutants of human respiratory syncytial virus. *J Virol* 2003; **77**: 11201–11211.
20 Tozawa H *et al.* Neutralizing activity of the antibodies against two kinds of envelope glycoproteins of Sendai virus. *Arch Virol* 1986; **91**: 145–161.
21 Tashiro M, Tobita K, Seto JT, Rott R. Comparison of protective effects of serum antibody on respiratory and systemic infection of Sendai virus in mice. *Arch Virol* 1989; **107**: 85–96.
22 Inoue M *et al.* Nontransmissible virus-like particle formation by F-deficient Sendai virus is temperature sensitive and reduced by mutations in M and HN proteins. *J Virol* 2003; **77**: 3238–3246.
23 Inoue M *et al.* A new Sendai virus vector deficient in the matrix gene does not form virus particles and shows extensive cell-to-cell spreading. *J Virol* 2003; **77**: 6419–6429.
24 Inoue M *et al.* Recombinant Sendai virus vectors deleted in both the matrix and the fusion genes: efficient gene transfer with preferable properties. *J Gene Med*, published online 5 May 2004. doi:10.1002/jgm.597.
25 Kato A *et al.* Initiation of Sendai virus multiplication from transfected cDNA or RNA with negative or positive sense. *Genes Cells* 1996; **1**: 569–579.
26 Okada T *et al.* Efficient directional cloning of recombinant adenovirus vectors using DNA–protein complex. *Nucleic Acids Res* 1998; **26**: 1947–1950.
27 Okada T *et al.* Adeno-associated viral vector-mediated gene therapy of ischemia-induced neuronal death. *Methods Enzymol* 2002; **346**: 378–393.
28 Nakano T, Kodama H, Honjo T. Generation of lympho-hematopoietic cells from embryonic stem cells in culture. *Science* 1994; **265**: 1098–1101.
29 Li F *et al.* Bone morphogenetic protein 4 induces efficient hematopoietic differentiation of rhesus monkey embryonic stem cells *in vitro*. *Blood* 2001; **98**: 335–342.
30 Sekhsaria S *et al.* Peripheral blood progenitors as a target for genetic correction of $p47^{phox}$-deficient chronic granulomatous disease. *Proc Natl Acad Sci USA* 1993; **90**: 7446–7450.
31 Lee SH *et al.* Efficient generation of midbrain and hindbrain neurons from mouse embryonic stem cells. *Nat Biotechnol* 2000; **18**: 675–679.
32 Johe KK *et al.* Single factors direct the differentiation of stem cells from the fetal and adult central nervous system. *Genes Dev* 1996; **10**: 3129–3140.
33 Takada T *et al.* Monkey embryonic stem cell lines expressing green fluorescent protein. *Cell Transplant* 2002; **11**: 631–635.

Hematopoietic Microchimerism in Sheep After In Utero Transplantation of Cultured Cynomolgus Embryonic Stem Cells

Kyoko Sasaki,[1,6] Yoshikazu Nagao,[2] Yoshihiro Kitano,[3] Hideaki Hasegawa,[1,2] Hiroaki Shibata,[1] Masaaki Takatoku,[4] Satoshi Hayashi,[5] Keiya Ozawa,[4] and Yutaka Hanazono[1,7]

Background. Although directed differentiation of human embryonic stem (ES) cells would enable a ready supply of cells and tissues required for transplantation therapy, the methodology is limited. We have developed a novel method for hematopoietic development from primate ES cells. We first cultured cynomolgus monkey ES cells in vitro and transplanted the cells in vivo into fetal sheep liver, generating sheep with cynomolgus hematopoiesis.

Methods. Cynomolgus ES cells were induced to mesodermal cells on murine stromal OP9 cells with multiple cytokines for 6 days. The cells (average 4.8×10^7 cells) were transplanted into fetal sheep in the liver (n=4) after the first trimester (day 55–73, full term 147 days). The animals were delivered at full term, and two of them were intraperitoneally administered with human stem-cell factor (SCF).

Results. Cynomolgus hematopoietic progenitor cells were detected in bone marrow at a level of 1% to 2% in all four sheep up to 17 months posttransplant. No teratoma was found in the lambs. After SCF administration, the fractions of cynomolgus hematopoiesis increased by several-fold (up to 13%). Cynomolgus cells were also detected in the circulation, albeit at low levels (<0.1%).

Conclusions. Long-term hematopoietic microchimerism from primate ES cells was observed after in vitro differentiation to mesodermal cells, followed by in vivo introduction into the fetal liver microenvironment. The mechanism of such directed differentiation of ES cells remains to be elucidated, but this procedure should allow further investigation.

Keywords: Primate embryonic stem cells, In utero transplantation, Hematopoietic microchimerism, Sheep.

(*Transplantation* 2005;79: 32–37)

A major barrier for most tissue or cellular transplantation therapies is the shortage of donors. Because human embryonic stem (ES) cell lines have dual abilities to proliferate indefinitely and differentiate into multiple tissue cells (*1, 2*), directed differentiation of human ES cells into functionally defied tissue types is a goal in providing an inexhaustible and potentially customized supply of transplantable cells or tissues. Clearly directed differentiation of ES cells is still in its infancy, and the methodology is quite limited. Many researchers have studied in vitro specific differentiation programs through manipulation of the cytokine milieu, cellular microenvironment, and conditional activation of specific gene expression (*3–5*). On the other hand, we and other groups have shown a line of evidence that undifferentiated ES cells respond to local cues after transplantation and differentiate into site-specific cells in rodent and nonhuman primate allogeneic transplantation models (*6, 7*). These studies have highlighted the importance of the in vivo local microenvironment for directed differentiation of ES cells. ES cells can be induced to differentiate into specific cells if exposed to the proper microenvironment. In this study, we have tried to use the in vivo fetal sheep liver microenvironment for hematopoietic development from primate ES cells.

Sheep in utero transplantation has been used as an assay system for human hematopoiesis (*8*). The fetal sheep is immunologically tolerant of allogeneic skin grafts or xenogeneic human hematopoietic cells before 75 days of gestation, which allows avoidance of the immunologic barriers present in postnatal models (*8–10*). In this model, long-term human/sheep hematopoietic chimeras have been established after the transplantation of human hematopoietic stem cells into the fetal sheep at a preimmune stage (*8*). It has also been reported that human mesenchymal stem cells engraft and show site-specific differentiation after in utero transplantation in sheep (*11*).

We have used nonhuman primate (cynomolgus monkey) ES cells (*12*) because this is the most faithful model for human ES cells for generating hematopoietic chimera in sheep. We first cultured cynomolgus ES cells in vitro to differentiate into mesodermal cells and introduced the cells into fetal sheep liver after the first trimester. Fetal liver is a hematopoietic organ at this stage of fetuses. We then examined the in vivo fate of transplanted cell progeny long term.

MATERIALS AND METHODS

Cell Preparation

Cynomolgus macaque ES cells (CMK6) were maintained on a feeder layer of mitomycin C (Kyowa, Tokyo, Japan) treated mouse (BALB/c, Charles River Japan,

This study was supported by the Ministry of Education, Culture, Sports, Science and Technology of Japan.

[1] Division of Regenerative Medicine, Center for Molecular Medicine, Jichi Medical School, Tochigi, Japan.
[2] Department of Agriculture, Utsunomiya University, Tochigi, Japan.
[3] Department of Surgery, National Center for Child Health and Development, Tokyo, Japan.
[4] Division of Hematology, Department of Internal Medicine, Jichi Medical School, Tochigi, Japan.
[5] Department of Obstetrics and Gynecology, National Center for Child Health and Development, Tokyo, Japan.
[6] Department of Plastic and Reconstructive Surgery, Faculty of Medicine, University of Tokyo, Tokyo, Japan.
[7] Address correspondence to: Dr. Yutaka Hanazono, Associate Professor, Head, Division of Regenerative Medicine, Jichi Medical School, 3311–1 Yakushiji, Minamikawachi, Tochigi 329–0498, Japan. E-mail: hanazono@jichi.ac.jp.

Received 3 March 2004. Revision requested 7 April 2004 and 10 June 2004. Accepted 19 July 2004.

ISSN 0041-1337/05/7901-32
DOI: 10.1097/01.TP.0000144058.87131.C5